Int J Hum Genet, 18(2): 95-101 (2018)
DOI: 10.31901/24566330.2018/18.2.692

Investigation of lncRNA Biomarkers in Postmenopausal Osteoporosis Using an lncRNA-Mediated, Competitive Endogenous RNA Network

Hong-Zhuan Li, Ji-Rong Zhao, Fei Li, Jiu-Xia Wang and Hong Zhou

Department of Orthopedics, Gansu Provincial Hospital of TCM, Lanzhou, 730050, Gansu Province, China

KEYWORDS Biomarkers for Postmenopausal Osteoporosis. Competitive Endogenous Rnas. Long Non-coding RNA Biomarker. Module. Molecular Mechanism

ABSTRACT In the present study, the researchers aimed to investigate long non-coding RNA (lncRNA) biomarkers for postmenopausal osteoporosis (PO) based on an lncRNA-mediated competitive endogenous RNAs (ceRNAs) network (LMCN). The LMCN was constructed by integration of lncRNA and mRNA expression profiles, miRNA-target interactions and Pearson correlation coefficient (PCC) algorithm. Topological degree centrality analysis was conducted on the LMCN to investigate optimal lncRNAs. Subsequently, a synergistic, competing module which correlated to optimal lmcRNAs closely was extracted from the LMCN utilizing the Biclique algorithm. As a result, the LMCN was comprised of 50 lncRNAs, 1,205 mRNAs and 1,393 ceRNA interactions, from which a module with 13 lncRNAs, 54 mRNAs and 117 interactions was extracted. The top 5 lncRNAs in descending order of degree were defined as optimal lncRNA biomarkers. In summary, the findings provide lncRNA biomarkers for target treatment and detection of PO patients, and give great insights to revealing the molecular mechanism underlying this disease.

INTRODUCTION

Broadly speaking, non-coding RNAs (ncRNAs) can be devided into small ncRNAs (< 200 nucleotides, containing microRNAs, piRNAs and siRNAs) and long non-coding (lncRNAs) (> 200 nucleotides) (Wang et al. 2015). More specifically, microRNAs (miRNAs) palys the role in the post-transcriptional level by way of destabilizing and repressing target mRNAs, which were related to the miRNA-induced silencing complex (Bartel 2014). Whereas lncRNAs are involved in many kinds of biological functions, for instance the regulation of cell apoptosis and invasion, chromatin modification, genomic imprinting and reprogramming of induced pluripotent stem cells (Wang and Chang 2011; Khaitan et al. 2011; Loewer et al. 2010). MiRNAs have been the most widely studied and involved in a variety of human diseases. By comparison, only a small amount of lncRNAs have been functionally characterized.

Address for correspondence:
Hong-Zhuan Li
Department of Orthopedics, Gansu Provincial Hospital of TCM,
No.418 on Guazhou Road, Qilihe District,
Lanzhou, 730050, Gansu Province, China
Telephone: 86-0931-2615729
Fax: 86-0931-2687021
E-mail: hongzhuanligansu@163.com

Recent researches have demonstrated that lncRNAs could take part in competing endogenous RNAs (ceRNAs) regulations for purpose of communicate with other RNA transcripts simultaneously (Ebert and Sharp 2010; Arvey et al. 2010). By sharing common miRNA-binding sites with messenger RNAs (mRNAs), lncRNAs compete with miRNA target genes for miRNA molecules, thereby relieving miRNA-mediated target repression (Wang et al. 2015). Thus, interaction between miRNA and lncRNA might be divided into direct connection and undirected regulation though competing interactions (Thum and Condorelli 2015). However, the functions of lncRNAs in postmenopausal osteoporosis (PO) are not well characterized, and the identification of lncRNA biomarkers is challenging.

Objectives

The researchers proposed an lncRNA-mediated ceRNA network (LMCN) to investigate lncRNA biomarkers for PO. By integrating lncRNA and mRNA expression profiles, miRNA-target interactions and Pearson correlation coefficient (PCC) algorithm, the LMCN was constructed. Subsequently, topological centrality analysis was performed to explore optimal lncRNAs in the LMCN. A synergistic, competing module was extracted from the LMCN utilizing the Bi-

clique algorithm to investigate significant mRNAs connected to the optimal lncRNAs. Finally, pathway enrichment analysis was carried out on mRNAs and lncRNAs in the module. These biomarkers might be potential markers for target treatment of PO, and give a hand for revealing pathological mechanism underlying this disease.

METHODOLOGY

Expression Profiles of lncRNA, miRNA and mRNA

To our best knowledge, small non-coding RNAs (sRNAs) target Base (starBase) facilitates comprehensive exploration of miRNA-target interaction manually curated from published studies (Yang et al. 2011). Specifically, starBase v2.0 (http://starbase.sysu.edu.cn/) systematically identifies the RNA-RNA and protein-RNA interaction networks from 108 CLIP-Seq (PAR-CLIP, HITS-CLIP, iCLIP, CLASH) datasets (Li et al. 2013). Hence, in this paper, the researchers recruited the comprehensive experimentally supported miRNA-mRNA and miRNA-lncRNA interactions from the starBase v2.0, termed background interactions.

An independent lncRNA and mRNA expression dataset of PO (E-GEOD-56814) was collected from the Affymetrix GeneChip Human Exon 1.0 ST Array version 1 [HuEx-1_0-st-v1] in the ArrayExpress database (http://www.ebi.ac.uk/arrayexpress/). E-GEOD-56814 was consisted of 73 samples, including 31 premenopausal samples regarded as normal controls and 42 postmenopausal samples attributed to PO patients. After performing standard pre-treatments and converting data on probe level into gene symbols, a total of 14,451 genes were detected in the gene expression data.

For purpose of making background interactions more correlated with PO, the researchers mapped genes in the gene expression data to miRNA-mRNA and miRNA-lncRNA interactions, and took the intersections. As a result, a new expression dataset with 8,471 mRNAs and 51 lncRNAs was identified. Afterwards, interactions containing any gene of the new expression dataset were extracted from the background interactions. In consequence, total 265,782 miRNA-mRNA or miRNA-target interactions, and 598 lncRNA-miRNA interactions were determined for subsequent analysis.

Identify ceRNA Interactions

In order to appraise competing lncRNA-mRNA reciprocity, a hypergeometric test was executed for each of them to screen potential ceRNA interactions (Sumazin et al. 2011), which enabled assessment of the significance of the common miRNAs between each lncRNA and mRNA. In order to evaluate the enrichment significance for interactions, the *P* value was calculated by utilizing the following formula:

$$P = \sum_{i=c}^{\min(K,n)} \frac{\binom{K}{i}\binom{N-K}{n-i}}{\binom{N}{n}}$$

Where *N* was the total number of miRNAs used to predict targets; *K* was the number of miRNAs that interacted with the chosen gene of interest; *n* was the number of miRNAs that interacted with the candidate ceRNA of the chosen gene; and *c* is the common miRNA number between lncRNAs and mRNAs. Of note, numerous miRNAs part of the same family were combined into one, and the hypergeometric test counted every miRNA family only once. False discovery rate (FDR) was used to correct P values based on Benjamini and Hochberg method (Liu et al. 2018a; Liu et al. 2018b). Besides, $P < 0.01$ was set as the threshold.

Construction of LMCN

With an attempt to evaluate interacted strengths of ceRNA interactions, PCC algorithm was implemented to measure the co-expression probability for the competing lncRNA-mRNA pairs. Supposing that *x* and *y* stood for two variables of a ceRNA interaction under a specific condition, the PCC was computed as following:

$$PCC(x,y) = \frac{cov(x,y)}{\sigma_x \sigma_y}$$

Of which cov(*x*, *y*) was the covariance of *x* and *y*; σ_x and σ_y were the standard deviations for *x* and *y*, respectively. Note that the PCC for a ceRNA interaction across normal and PO condition was different. The absolute difference of PCC value across normal and PO condition was defined as a weight for this ceRNA interaction and only ceRNA interactions with weight > 0.5 were reserved. When integrating these reserved interactions with miRNA-target interactions and gene expression data, a LMCN for PO was visualized by Cytoscape software v3.1.0 (http://www.cytoscape.org/) (Morris et al. 2014).

Network Topological Analysis

A fundamental issue in network analysis is the importance of determining a particular vertex or an edge in a network (Bader and Madduri 2006; Liu et al. 2018c). With the help of quantifying centrality and connectivity, the researchers could identify portions of the network that may act an interesting part. Researchers have revealed that topological centrality is shown to be effective for identifying essential molecules in well-characterized interaction networks (Prifti et al. 2010). In order to cotton on the functionality of gene signatures, the researchers characterized the biological importance of nodes in the LMCN using index of topological analysis (degree), and defined the top 5 ones with high degree as potential optimal biomarkers for PO patients. Degree quantifies the local topology of each nodethrouth summing up its adjacent nodes numbers (Martinez et al. 2018; McLaughlin et al. 2017). It gives a simple count of the number of interactions for a given node. What's more, the relationship between the number of nodes and degree distribution was also investigated. The fitting coefficient R^2 of the power-law $y=ab^x$ of the LMCN was investigated, separately. Since networks in general are modular and scale-free, a good R^2 indicates that the network has a power-law (or scale-free) degree distribution (Garcia-Heredia et al. 2015). Besides, Network Analyzer 2.7 plugin in Cytoscape v3.1.0 (Morris et al. 2014) was employed for the evaluation of topological parameter.

Extraction of Synergistic, Competing Modules

The LMCN offered a comprehensive view of all potential ceRNA interactions, whereas a network with too large scale might be too generic, and a sub-network might exhibit more details of how the lncRNAs synergized with competing mRNAs, especially for the optimal lncRNAs. Hence, in this paper, a synergistic, competing lncRNA module (sub-LMCN) was extracted from the LMCN using the Biclique algorithm. Importantly, in competing module, which was a complete bipartite graph, an edge was realized from every vertex of a miRNA set to every vertex of a target gene set. In particular, a complete bipartite graph is a graph whose vertices can be partitioned into two subsets V_1 and V_2 such that no edge has both endpoints in the same subset, and every possible edge that could connect vertices in different subsets is part of the graph (Ren et al. 2018). That is, it is a bipartite graph (V_1, V_2, M) such that for every two vertices $v_1 \varepsilon V_1$ and $v_2 \varepsilon V_2$, v_1v_2 is an edge in M. Every two graphs with the same notation are isomorphic.

Pathway Enrichment Analysis

As described above, the researchers obtained lncRNAs and mRNAs which enriched in the module. Based on these lncRNAs and mRNAs, pathway enrichment analysis was conducted to explore significant pathways for PO according to Kyoto Encyclopedia of Genes and Genomes (KEGG, http://www.genome.jp/kegg/) implemented in Database for Annotation, Visualization and Integrated Discovery (DAVID, https://david.ncifcrf.gov/) (Huang et al. 2008; Shi et al. 2018). Furthermore, the Fisher's exact test (Vieira et al. 2018) was employed to identify the significant pathways between PO patients and normal controls. The threshold of significance was defined as $P < 0.01$ which were adjusted by false discovery rate (FDR) correction based on Benjamini and Hochberg method (Wang et al. 2018).

RESULTS

ceRNA Interactions

Using 265,782 miRNA-target interactions and 598 lncRNA-miRNA interactions, the researchers identified competing lncRNA-mRNA interactions or ceRNA interactions based on the hypergeometric test. During this step, a P value was implemented to compute the significance of the shared miRNAs between each lncRNA-mRNA pair. When setting the thresholding as $P < 0.01$, total 34,586 ceRNA interactions involved in 51 lncRNAs and 8,125 mRNAs were obtained totally for the subsequent study.

LMCN

To the researchers' knowledge, a number of ceRNAs might be co-expressed in certain tissues and exhibit activities in specific diseases (Wang et al. 2015). With the goal of determining active ceRNA pairs in PO, a weight was calculated for each ceRNA pair identified above dependent on the PCC. Ultimately, significantly co-

expressed lncRNA-mRNA ceRNA pairs with weight > 0.5 were reserved to construct the LMCN and were graphically visualized by Cytoscape v3.1.0. There were 50 lncRNAs, 1,205 mRNAs and 1,393 ceRNA interactions in the LMCN. Subsequently, the topological degree centrality analysis was counted for each node in the LMCN to explore its biological importance in the progression of PO. As shown in Figure 1, topological analysis revealed specific properties of the lncRNA-mediated ceRNA network (LMCN). The node degree distribution of the lncRNA nodes ($R^2 = 0.97037$), the mRNA nodes ($R^2 = 0.99991$), and the entire nodes ($R^2 = 0.99988$) revealed power law distributions, which indicated that the PO-associated LMCN was a scale-free network. Meanwhile, the fitting formula for each curve also was displayed in the figure. Specifically, LINC00173 (degree = 207), BAIAP2-AS1 (degree = 184), EPB41L4A-AS1 (degree = 98), LINC00319 (degree = 90) and ENTPD1-AS1 (degree = 71) were the most significant lncRNAs with higher degree than the others, and denoted as optimal lncRNAs.

Synergistic, Competing Module

While the LMCN could afford a global view of all possible competing ceRNA interactions to detect functional regulations of the lncRNAs, the partial sub-network might reveal a more detailed and representative diagram of how lncRNAs synergized with competing mRNAs. As a consequence, synergistic, competing modules were extracted from the LMCN by utilizing the Biclique algorithm. A total of 1 module was captured, which was comprised of 13 lncRNAs, 54 mRNAs and 117 interactions, as illustrated in Figure 2. LncRNAs were shown as light color nodes, whereas mRNAs were described as deep color nodes. Note that the thickness of an edge indicated its weight value. The thicker of an edge, the higher weight of its weight, and the more important of its connected nodes were. In detail, the researchers uncovered that LINC00173 competed with 21 mRNAs (degree = 21), especially BCL3. The weight between LINC00173 and BCL3 (weight = 0.83) was the highest of all, which indicated that the strength of this interaction was the strongest. And the weight for lncRNA ENTPD1-AS1 and mRNA PPIF was the second of 0.82.

KEGG Pathways

For purpose of investigating functional gene sets for lncRNAs and mRNAs in the synergistic, competing module, KEGG pathway enrichment analysis was conducted. The results showed that 8 significant pathways were obtained under the threshold of $P < 0.01$. As seen in Table 1, Cell cycle (P = 2.54E-19), Adherens junction (P = 7.30E-04), Neuroactive ligand-receptor interaction (P = 9.84E-04), ErbB signaling pathway (P = 1.72E-05), Protein export (P = 4.43E-05) were the top five pathways in descending order of P value for PO.

DISCUSSION

As a silent skeletal disorder, PO is characterized by impaired bone strength, which can easily lead to an increased risk of fracture (Watts et al. 2010). A lack of endogenous oestrogen in menopausal females was its direct cause (Carlin et al. 2017). Specifically, hormonal changes,

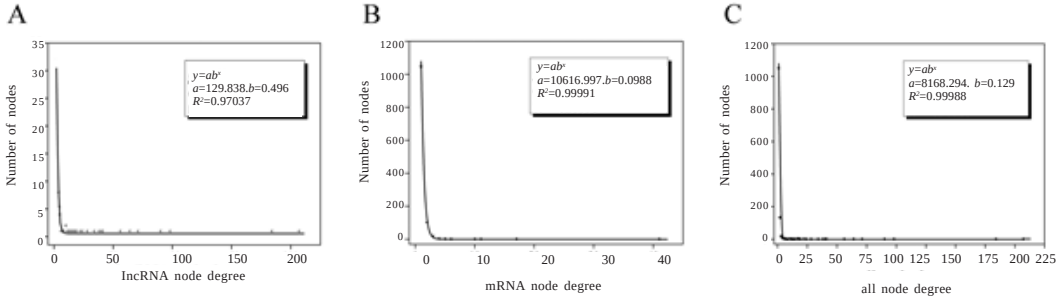

Fig. 1. Topological analysis revealed specific properties of the lncRNA-mediated ceRNA network (LMCN). The lncRNA nodes (A), mRNA nodes (B) and the entire network (C) reflected a power-law distribution

Table 1: KEGG pathway enriched by lncRNAs and mRNAs in competing module

Pathway ID	*Term*	*P value*
hsa03060	Cell cycle	2.54E-19
hsa04012	Adherens junction	7.30E-04
hsa04080	Neuroactive ligand-receptor interaction	9.84E-04
hsa04144	ErbB signaling pathway	1.72E-05
hsa04110	Protein export	4.43E-05
hsa04114	Endocytosis	6.71E-05
hsa04520	Oocyte meiosis	1.69E-03
hsa04740	Olfactory transduction	1.87E-03

which proceed over all perimenopause and the immediate postmenopausal years, stimulate the receptor activator of nuclear factor-κβ (*RANK*) and its ligand (*RANKL*) production (both directly and indirectly), leading to accelerated bone loss (Stuss et al. 2013). Low bone mass density and fracture are two major manifestations of PO patients clinically, and even vertebral compression fractures may happen during routine daily activities without a specific fall or injury (Unni et al. 2015). In consequence, PO imposes a significant burden on both the individual and society. Fortunately, it can be prevented, diagnosed, and treated before fractures occur (Cosman et al. 2014). Hence providing effective biomarkers for PO has become more and more important and urgent.

To the best of the researchers' knowledge, miRNAs are likely regulated by other RNAs that contain complementary miRNA binding sites such as lncRNAs and mRNAs, and these ceRNAs mutually manage their expressed levels by competing mechanisms (Cao et al. 2016), which are crucial to various disease physiological and pathological processes. What's more, lncRNAs have been identified in RNA-RNA cross-talk networks as competitors of mRNAs for miRNA binding, thereby regulating mRNA expression levels through an indirect post-transcriptional mechanism (Salmena et al. 2011). Therefore, in the present research, the researchers have in-

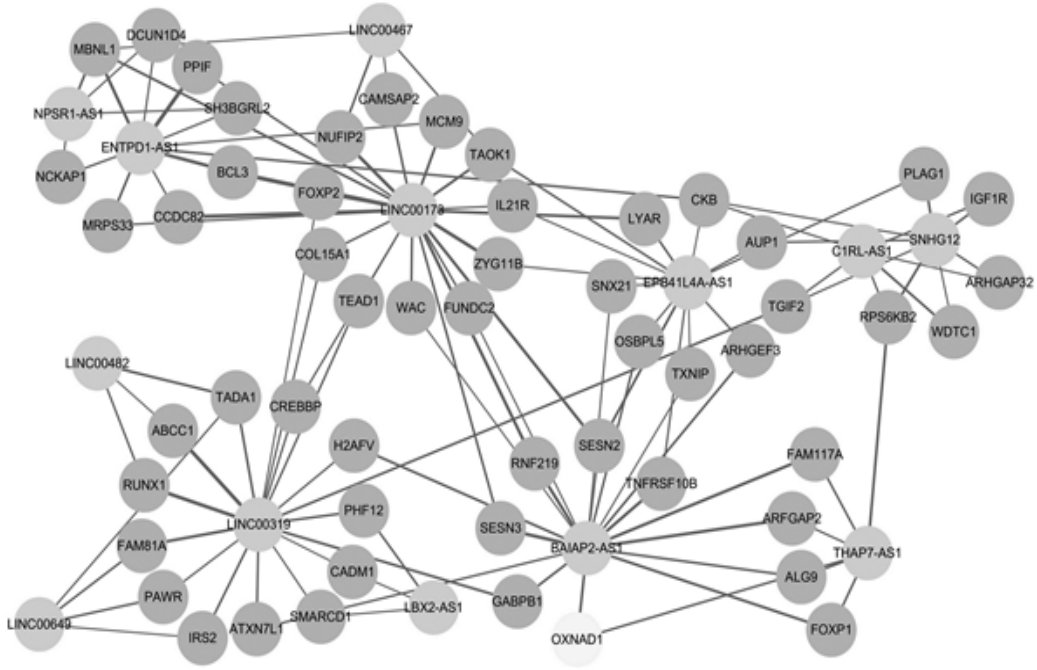

Fig. 2. The synergistic, co-competing module extracted from the lncRNA-mediated ceRNA network (LMCN). LncRNAs were shown as yellow nodes, whereas mRNAs were described as blue nodes. The thickness of an edge represented its weight value, the thicker of an edge, the higher weight it had
Source: Author

vestigated lncRNA biomarkers for PO based on the LMCN. Construction of the LMCN integrated lncRNA and mRNA expression data, miRNA-target interactions and PCC algorithm, which enhanced the reliability and feasibility of the network. There were 50 lncRNAs, 1,205 mRNAs and 1,393 ceRNA interactions in the LMCN for PO. Particularly, the lncRNA nodes were usually located in the central area of the network, while the mRNAs nodes were typically in the outside layer. Besides, Tay et al. reported that crosstalk between ceRNAs could be regulated through multiple layers of gene that concerned interactions of different RNA species (Tay et al. 2014). On the basis of ceRNA regulatory behavior, LncRNAs in the LMCN were more likely to have central regulatory roles than mRNAs, especially those with high degree. In addition, the degree distribution of lncRNA, mRNA, and entire nodes in LMCN suggested power law distributions, showing that the PO-associated LMCN was a scale-free network. In summary, the LMCN resembled many biological networks and was well structured by a core set of lncRNA-mRNA competing principles into structured instead of random networks (Desai et al. 2017).

In spite of large-scale protein interaction data is keeping accumulated with the growth of high throughput technology, a set number of significant nodes and interactions are not tested (Nibbe et al. 2011). Besides, a network with too large-scale might be too generic and not representative. This difficulty might be resolved by using sub-networks or modules of the complex network (Wu et al. 2014). Hence a synergistic, competing module was extracted from the LMCN utilizing the Biclique algorithm to provide a detailed and specific graph of important lncRNA activities. It was comprised of 13 lncRNAs, 54 mRNAs and 117 interactions. Furthermore, its degree distribution had a power law, which suggested the module was a scale-free network. Interestingly, the top 5 lncRNAs with high degree in the LMCN were considered to be optimal lncRNAs for PO, LINC00173, BAIAP2-AS1, LINC00319, EPB41L4A-AS1, and ENTPD1-AS1.

Generally speaking, lncRNAs take prominent effect in competitive interactions, leading to correspond changes in miRNA and gene expressions. While roles for lncRNAs as drivers of tumor suppressive and oncogenic functions have appeared in prevalent cancer types (Prensner and Chinnaiyan 2011), few researchers pay attention to dissect lncRNA functions in PO. In this study, it is the first time to reveal novel lncRNA biomarkers for PO. For example, LINC00173 (long intergenic non-protein coding RNA 173) played a role that predicted individuals at potential risk for developing pre-osteoarthritis based on screening of genetic risk-alleles associated with pre-osteoarthritis (Farooq et al. 2016). BAIAP2-AS1 (brain-specific angiogenesis inhibitor associated protein 2 antisense RNA 1) offered resource for further search of biomarkers and therapeutic targets of hepatitis B virus -related hepatocellular carcinoma (Gong et al. 2016).

CONCLUSION

In summary, the researchers' identified 5 lncRNA biomarkers for PO. The findings provide potential molecular markers for target treatment and detection of PO, and give great insights to revealing the molecular mechanism underlying this disease. Whereas future studies should focus on the experimental validations of these lncRNAs.

RECOMMENDATIONS

However, there are some limitations in this experiment. For example, the sample size is small, and subsequent experiments need to increase the sample size for the further study. Moreover, clinical trials are also needed for verification.

ACKNOWLEDGEMENT

This study was supported by Lanzhou Science and Technology Planning Project (grant No. 2014-1-9).

REFERENCES

Arvey A, Larsson E, Sander C, Leslie CS, Marks DS 2010. Target mRNA abundance dilutes microRNA and siRNA activity. *Molecular Systems Biology,* 6: 363.

Cao Y, Wang P, Ning S, Xiao W, Xiao B, Li X 2016. Identification of prognostic biomarkers in glioblastoma using a long non-coding RNA-mediated, competitive endogenous RNA network. *Oncotarget,* 7(27): 41737-41747.

Carlin DE, Paull EO, Graim K, Wong CK, Bivol A, Ryabinin P, Ellrott K, Sokolov A, Stuart JM 2017. Prophetic granger causality to infer gene regulatory networks. *Scientific Reports,* 12: e0170340.

Cosman F, De Beur S, Leboff M, Lewiecki E, Tanner B, Randall S, Lindsay R 2014. Clinician's guide to preven-

tion and treatment of osteoporosis. *Osteoporosis International,* 25: 2359-2381.
Desai JS, Sartor RC, Lawas LM, Jagadish SVK, Doherty CJ 2017. Improving gene regulatory network inference by incorporating rates of transcriptional changes. *Sci Rep,* 7(1): 17244.
Ebert MS, Sharp PA 2010. Emerging roles for natural microRNA sponges. *Current Biology,* 20: 858-861.
Farooq RM, Sandell LJ, Zhang B, Wright RW, Brophy RH 2016. RNA microarray analysis of macroscopically normal articular cartilage from knees undergoing partial medial meniscectomy: Potential prediction of the risk for developing osteoarthritis. *PLoS One,* 11.
Gong X, Wei W, Chen L, Xia Z, Yu C 2016. Comprehensive analysis of long non-coding RNA expression profiles in hepatitis B virus-related hepatocellular carcinoma. *Oncotarget,* 7(27): 42422-42430.
Khaitan D, Dinger ME, Mazar J, Crawford J, Smith MA, Mattick JS, Perera RJ 2011. The melanoma-upregulated long noncoding RNA SPRY4-IT1 modulates apoptosis and invasion. *Cancer Research,* 71: 3852-3862.
Li JH, Liu S, Zhou H, Qu LH, Yang JH 2013. starBase v2.0: Decoding miRNA-ceRNA, miRNA-ncRNA and protein-RNA interaction networks from large-scale CLIP-Seq data. *Nucleic Acids Research,* 42: 92-97.
Liu A, Le A, Zhang J, Wong C, Wong C, Henry L, Nguyen MH 2018a. Increasing co-morbidities in chronic hepatitis B patients: Experience in primary care and referral practices during 2000-2015. *Clinical and Translational Gastroenterology,* 9: 141.
Liu C, Wu W, Shang H, Lin S, Xun Z, Huang E, Lin J, Yang B, Ou Q 2018b. Prediction value of serum HBV large surface protein in different phases of HBV infection and virological response of chronic hepatitis B patients. *Clinica Chimica Acta; International Journal of Clinical Chemistry,* 481: 12-19.
Loewer S, Cabili MN, Guttman M, Loh YH, Thomas K, Park IH, Garber M, Curran M, Onder T, Agarwal S 2010. Large intergenic non-coding RNA-RoR modulates reprogramming of human induced pluripotent stem cells. *Nature Genetics,* 42: 1113-1117.
Martinez CA, Khare K, Elzo MA 2018. BIBI: Bayesian inference of breed composition. *Journal of Animal Breeding and Genetics = Zeitschrift Fur Tierzuchtung und Zuchtungsbiologie,* 135: 54-61.
Mclaughlin HP, Cherney B, Hakovirta JR et al. 2017. Phylogenetic inference of Coxiella burnetii by 16S rRNA gene sequencing. *PLoS One,* 12: e0189910.
Morris JH, Wu A, Doncheva NT, Albrecht M, Ferrin TE 2014. SetsApp: Set operations for cytoscape nodes and edges. *F1000 Research,* 3: 149-149.
Nibbe RK, Chowdhury SA, Koyut RKM, Ewing R, Chance MR 2011. Protein–protein interaction networks and subnetworks in the biology of disease. *Wiley Interdisciplinary Reviews: Systems Biology and Medicine,* 3: 357-367.
Prensner JR, Chinnaiyan AM 2011. The emergence of lncRNAs in cancer biology. *Cancer Discovery,* 1: 391-407.
Prifti E, Zucker J-D, Clement K, Henegar C 2010. Interactional and functional centrality in transcriptional co-expression networks. *Bioinformatics,* 26: 3083-3089.
Ren G, Liu X, Yu Z, Li J, Niu F, Jin T, Liu J, Chen M 2018. Association of TERT polymorphisms with chronic hepatitis B in a Chinese Han population. *Oncotarget,* 9: 9199-9205.
Salmena L, Poliseno L, Tay Y, Kats L, Pandolfi PP 2011. A ceRNA hypothesis: The Rosetta stone of a hidden RNA language? *Cell,* 146: 353-358.
Shi Y, Liu W, He M 2018. Proteome and transcriptome analysis of ovary, intersex gonads, and testis reveals potential key sex reversal/differentiation genes and mechanism in scallop chlamys nobilis. *Mar Biotechnol,* 20(2): 220-245.
Stuss M, Rieske P, Ceg³owska A, Stepieñ-K³os W, Liberski PP, Brzeziañska E, Sewerynek E 2013. Assessment of OPG/RANK/RANKL gene expression levels in peripheral blood mononuclear cells (PBMC) after treatment with strontium ranelate and ibandronate in patients with postmenopausal osteoporosis. *The Journal of Clinical Endocrinology and Metabolism,* 98: E1007-E1011.
Sumazin P, Yang X, Chiu HS, Chung WJ, Iyer A, Llobetnavas D, Rajbhandari P, Bansal M, Guarnieri P, Silva J 2011. Abstract 4186: An extensive microRNA-mediated network of RNA-RNA interactions regulates established oncogenic pathways in glioblastoma. *Cancer Research,* 147: 370-381.
Tay Y, Rinn J, Pandolfi PP 2014. The multilayered complexity of ceRNA crosstalk and competition. *Nature,* 505: 344-352.
Thum T, Condorelli G 2015. Long noncoding RNAs and microRNAs in cardiovascular pathophysiology. *Circulation Research,* 116: 751-762.
Unni S, Yao Y, Milne N, Gunning K, Curtis JR, Lafleur J 2015. An evaluation of clinical risk factors for estimating fracture risk in postmenopausal osteoporosis using an electronic medical record database. *Osteoporosis International,* 26: 581-587.
Vieira WAS, Lima WG, Nascimento ES 2018. The impact of phenotypic and molecular data on the inference of colletotrichum diversity associated with Musa. *Mycologia,* 109(6): 912-934.
Wang KC, Chang HY 2011. Molecular mechanisms of long noncoding RNAs. *Molecular Cell,* 43: 904-914.
Wang P, Ning S, Zhang Y, Li R, Ye J, Zhao Z, Zhi H, Wang T, Guo Z, Li X 2015. Identification of lncRNA-associated competing triplets reveals global patterns and prognostic markers for cancer. *Nucleic Acids Research,* 43: 3478-3489.
Wang R, Xie R, Song Z 2018. Circulating regulatory Tfh cells are enriched in patients with chronic hepatitis B infection and induce the differentiation of regulatory B cells. *Experimental Cell Research,* 365(2): 171-176.
Watts NB, Bilezikian JP, CamaCho PM, Greenspan SL, Harris ST, Hodgson SF, Kleerekoper M, Luckey MM, Mcclung MR, Pollack RP 2010. American association of clinical endocrinologists' medical guidelines for clinical practice for the diagnosis and treatment of postmenopausal osteoporosis. *Endocrine Practice,* 16(Suppl 3): 1-37.
Wu Y, Jing R, Jiang L, Jiang y, Kuang Q, Ye L, Yang L, Li Y, Li M 2014. Combination use of protein-protein interaction network topological features improves the predictive scores of deleterious non-synonymous single-nucleotide polymorphisms. *Amino Acids,* 46: 2025-2035.
Yang JH, Li JH, Shao P, Zhou H, Chen YQ, Qu LH 2011. starBase: A database for exploring microRNA-mRNA interaction maps from Argonaute CLIP-Seq and Degradome-Seq data. *Nucleic Acids Research,* 39: 202-209.

Paper received for publication on March 2018
Paper accepted for publication on May 2018